Chapter 5
Conductive Adhesive Joint Reliability

Abstract There are two primary categories of electrically conductive adhesive (ECA): isotropic conductive adhesive (ICA) and anisotropic conductive adhesive (ACA), where ACAs are available as paste (ACP) or film (ACF). Both types conduct through metal filler particles in an adhesive polymer matrix.

This chapter presents an overview of the current status of understanding of conductive adhesives in various electronic packaging applications and of some fundamental issues relevant to their continuing development. It is organized with initial discussions of basic ECA concepts of structure-related properties, and how these are affected by material selection and processing, followed by general properties and reliability considerations.

5.1 Introduction to Conductive Adhesives

Recent environmental legislation has led to an increasing interest in the possibility of substituting electrically conductive adhesives (ECAs) for the traditional tin–lead solders in electronics manufacturing. The conductive adhesives mentioned in this chapter are not inherently conductive polymers that are extremely brittle and sensitive to oxidation. Instead, they are composites of insulating polymer matrix and conductive fillers. The polymer matrix and its characteristics are mostly responsible for the adhesive ability to bond and withstand mechanical stresses. The electrical conductivity of the adhesive depends particularly on the fillers. As a result, the electrical and mechanical properties can, to a large degree, be adjusted independently. Depending on the loading of fillers, conductive adhesives can be cataloged as isotropic conductive adhesive (ICA) and anisotropic conductive adhesive (ACA). Though not every adhesive currently has all of them, conductive adhesive interconnections offer the following advantages over traditional tin–lead solders:

- Low temperature processing
- Compatibility with a wide range of substrates
- No flux pretreatment or postcleaning procedures required

J. Liu et al., *Reliability of Microtechnology: Interconnects, Devices and Systems*,
DOI 10.1007/978-1-4419-5760-3_5,

- No lead or other toxic metals
- Finer pitch capability
- Solder mask not required

5.2 Isotropic Conductive Adhesive

ICAs have been successfully used for decades in the electronics industry as die-attach materials. Now new adhesives have been formulated to replace traditional solders in mainstream applications. The volume fraction of conductive fillers in the adhesive is between 20 and 35%, which is so high that the adhesive can conduct equally well in all directions. As a result, ICAs may be deposited only where electrical connects are required. In general, the conductivity of the adhesive improves with increasing filler loading, but at the expense of the adhesive becoming increasingly brittle. Copper, nickel, carbon, and silver are commonly used as conductive fillers. Silver is unique among these affordable fillers because of its good electrical performance, stability, and inherent conductivity of silver oxides. The matrix is mostly one- or two-component epoxies that can be cured with heat and/or IR radiation. However, polyimides, silicones, and thermoplastic adhesives can also be used as matrices.

The electrical conduction of an ICA joint is primarily established during cure. Instead of metallurgical connection, the joint conduction is based on mechanical contacts among conductive fillers (Fig. 5.1). Studies have shown that the conduction development during cure is accompanied by the decomposition of organic lubricants, which exposes the metallic surface of fillers, and the cure shrinkage, which brings fillers closer. However, the conduction mechanism of ICA is still not fully understood and which effect plays a dominant role is still open to question.

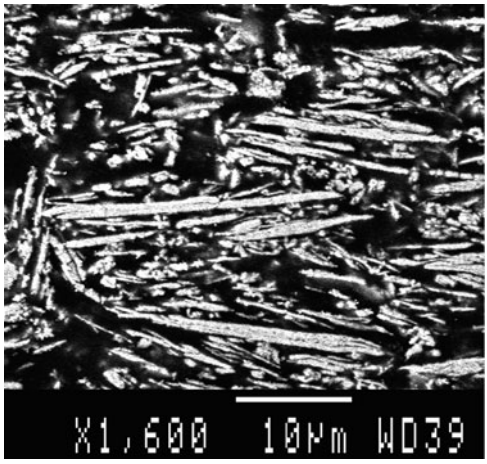

Fig. 5.1 Microstructure of an ICA showing silver fillers (*white*) embedded in the epoxy matrix (*black*)

After the adhesive is cured, the fillers are randomly distributed and form a network within the polymer matrix. By this network, electrons can flow from one adherent to the other across the filler contact points. The overall result is to create numerous electron pathways, but with each path made up of a large number of mechanical contacts. So any factors affecting intimate contacts among fillers will surely influence the performance and reliability of ICA interconnects.

Besides die attachment, ICAs are utilized in surface mount and flip-chip packages as alternatives to traditional solders. But, due to their low surface tensions, ICAs are not suitable for wave soldering. Despite the advantages of ICA interconnection, the wide use of this technology has not been adopted by the electronics industry. The main concern is the long-term reliability.

5.3 Reliability of ICA Interconnects

5.3.1 Effect of Metallization

To get a good adhesive joint, the adhesive must wet the bonding surface. A necessary condition for this is that the adhesive has lower surface tension than the bonding surface. Epoxy and polyimides are major polymers used as base matrices of ICAs. These materials have lower surface tension than Sn, Pb, Cu, Au, and Pd. Therefore, a good adhesive joint is expected when bonding on Sn, SnPb, Cu, AgPd, and Au surfaces.

As water molecules can easily penetrate through the adhesive and oxidize/hydrate the bonding surfaces, ICA joints with different metallizations have diverse reliability performances in high-humidity environments. Several investigations showed that joints with noble Au and AgPd metallizations had much less resistance increases compared with those with non-noble SnPb and Cu metallizations. The detailed failure mechanisms were investigated with transmission electron microscopy (TEM) and X-ray electron spectroscopy for chemical analysis (XPS/ESCA).

TEM observations on an adhesive joint with Sn37Pb metallization show that water has penetrated to the Sn37Pb surface after 1,000 h 85°C/85%RH test. As a result, oxygen signals can be detected with EDS analysis in TEM. The corresponding electron diffraction observes a diffused ring, which indicates that Pb was converted to an amorphous structure. So the reaction product is not crystalline PbO, but $Pb(OH)_2$ or other Pb oxides such as Pb_2O_3 and Pb_2O which have amorphous structures. The ESCA analysis on the Sn37Pb surface shows the chemical shift of the oxygen signals, confirming that the product is Pb-hydroxide. Due to the formation of amorphous $Pb(OH)_2$ which is an insulating compound and has a powdery structure, both electrical and mechanical properties of the ICA joint deteriorate. With the same metallization, Botter et al. [1] and Jagt [2] got similar resistance shift trends. But they focused more on tin oxidation according to electrochemical analysis.

TEM studies on an adhesive joint with copper metallization show the existence of the oxide layer on the Cu pad. The thickness is approximately 100 nm after 1,000 h 85°C/85%RH humidity test. The rings in the diffraction pattern obtained from the oxide layer indicate that the layer consists of fine crystalline grains. The radii of the rings correspond to the spacing of the crystallographic planes of Cu_2O. It is, therefore, concluded that the formed oxide is Cu_2O, which is a poor conductor. This helps to explain why the joint resistance increased after the humidity test.

Contrary to non-noble metallization, the electrical resistance of ICA joints mounting a gold-plated QFP80 component on an electroless Au-plated FR-4 board is quite stable in the 85°C/85% RH environment. No significant increase can be observed up to 2,000 h. Hence, it can be concluded that a noble metallization such as Au or Ag/Pd is preferable for normal ICAs. However, by adding corrosion inhibitors, some superior ICAs for pretinned metallization have been developed.

5.3.2 Effect of Curing Degree

There is no doubt that proper curing is very important for joint reliability. It was found that a minimum curing degree is required to provide a certain level of mechanical and electrical performance of adhesive joints, especially with non-noble metallizations. Once this is achieved, increasing curing times does not result in significant improvement.

Figure 5.2a shows the electrical resistance shifts of epoxy-based ICA joints after 1,000 h humidity test at 85°C/85%RH. These joints were on the Sn37Pb bonding surface and cured at 150°C for various time. The corresponding curing degrees were determined by differential scanning calorimetry (DSC) measurement as between 65 and 90%. Below a critical curing degree (for this adhesive, the critical curing degree is 77%), the electrical resistance of the joint increases significantly after humidity test. The reason is that an undercured epoxy can absorb a significant amount of water, which in turn causes oxidation/hydration of the Sn37Pb metallization. If a noble metallization such as AgPd is used, no electrical resistance shift

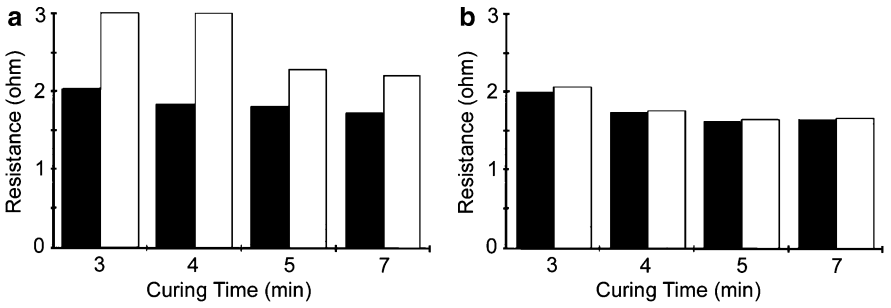

Fig. 5.2 Contact resistance shifts of ICA joints on (**a**) Sn37Pb and (**b**) Ag/Pd surfaces (*black*: before test; *white*: after test)

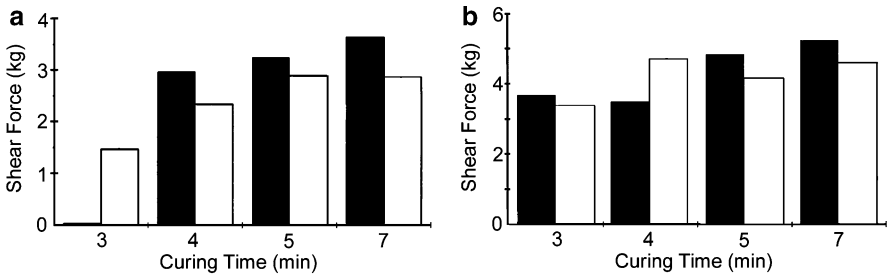

Fig. 5.3 Strength shifts of ICA joints on (**a**) Sn37Pb and (**b**) Ag/Pd surfaces (*black*: before test; *white*: after test). These joints were cured at 150°C for various time and then aged in the 85°C/85% RH environment

has been observed despite the fact that curing degree can be very low, as can be seen in Fig. 5.2b. These joints were cured at 150°C for various times and then aged in the 85°C/85%RH environment.

The same as electrical performance, once a critical curing degree is achieved (77%), the shear strength of the joint on the Sn37Pb bonding surface can be maintained at a constant level (Fig. 5.3a). However, on the noble metal bonding surface, the shear strength of the joint is almost independent of the curing degree in the range between 65 and 90%, as can be seen in Fig. 5.3b. These results also indicate that for conductive adhesive joining, noble metallization is preferable to non-noble metallization.

5.3.3 Impact Strength

Due to their high filler loading, many ICAs suffer from poor impact strength, which is one of the major drawbacks preventing their wide applications. Without adequate impact strength, ICA joints can hardly survive the significant shocks during assembly, handling, and usage. For bulk materials, impact performance is closely related to their fracture toughness and damping property. An adhesive with higher toughness and higher loss modulus normally has better impact performance. So a simple approach is to modify base epoxy resins with elastomers to improve the impact performance of ICAs. However, for adhesive joints, the adhesion strength between the adhesive and adherend is also very critical. Low impact strength can result from adhesive failure due to poor adhesion. Using conformal coating of surface mount devices is another practical way to improve the impact strength of the package.

To evaluate the impact performance of board-level packaging with ICAs, the National Center for Manufacturing Science (NCMS) has developed a special drop test. It involves dropping circuit boards onto hard ground from a height of 1.5 m and the sample surviving six drops is regarded to possess acceptable impact strength.

The test is easy to conduct, but only qualitative information could be supplied. Xu and Dillard [3] developed a novel falling wedge fracture test which is capable of quantitatively determining the impact strength of ICA joints. They used a modified double cantilever beam (DCB) specimen with ICA and PCB boards and measured the fracture energies under different test temperatures with this new test technique. The impact fracture energy was found to keep an approximately logarithmic relationship with the loss factor that in turn can serve as a good indicator of the impact performance of ICAs.

5.3.4 Failure Mechanisms

5.3.4.1 Cracking

Due to the temperature fluctuation caused by the circuit power on/off cycles, ICA interconnects have to sustain cyclic stresses from thermal expansion mismatch between the substrate and component, and thermomechanical fatigue cracking is considered as one of the primary failure mechanisms. Based on temperature cycling tests and cross-section observations, the fatigue cracking behavior of ICA joints of leadless chip resistors was investigated. Early cracking was detected at the top of the vertical adhesive/termination interface (Fig. 5.4a), which has been reported in [4]. With more cycles, cracks were observed at the inner end of the horizontal interface between adhesive and ceramic resistor body (Fig. 5.4b). As the number of cycles increased further, bulk cracking occurred around the knee of the joint (Fig. 5.4c). It appears that several microcracks nucleated simultaneously due to the debonding of silver flakes. Then they merged together and formed the main bulk crack that propagated from the component side to the board side. After initiation, both vertical and horizontal cracks propagated toward the knee area along the adhesive/termination interface and the final merging of the three cracks (Fig. 5.4d) resulted in a complete failure of the entire joint. Since most crack development occurs at the interface, the adhesion of ICA is critical to the joint reliability.

In humidity aging tests, cracks have always been found associated with electrical degradation of ICA joints. Li et al. [5] reported that cracks existed after cure and developed due to the humidity exposure, leading to deterioration in both mechanical strength and electrical conductivity. However, with similar observations, Botter et al. [1] attributed the cracking after humidity test to the formation of oxides. In a recent investigation on the degradation of ICA joints in humid environments, Xu et al. [6] concluded that moisture attack on the adhesive/metallization interface could be divided into three phases: displacing the adhesive due to high surface-free energy around the interface, hydrating the metal or metal oxide, and forming a weak boundary layer at the interface. If the attack occurs in the first phase, the fracture energy could recover to some extent after redrying at high temperature. However, the degradation becomes irreversible in the second phase.

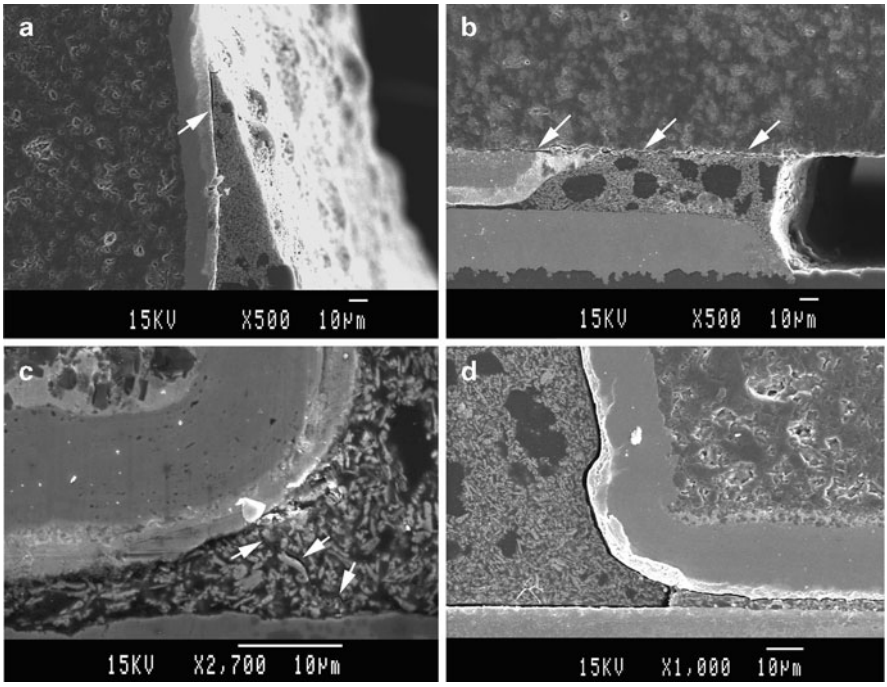

Fig. 5.4 Interfacial cracks initiated at (**a**) top and (**b**) inner ends of the adhesive/component interface; (**c**) bulk microcracks occurred around the knee of the joint. Cracks are indicated with *arrows*; (**d**) final merging of these cracks resulted in a complete failure of the entire joint

5.3.4.2 Formation of Oxides

When ICAs are used together with non-noble metallizations, the contact resistance will increase significantly during high temperature and high humidity aging. As discussed in Sect. 4.3.2, various oxides have been observed to form at the interface between ICA and metallization, which leads to resistance deterioration.

In climate tests (98%RH), Botter et al. found that tin oxides occurred only in the area where adhesive was attached. No visible oxidation was observed at the fully air-exposed area on the top of the resistor. So they proposed that the direct contact between the noble metal (Ag filler) and the non-noble metal (tin metallization), combined with absorbed water in the adhesive, formed a local electrochemical cell, which corroded the non-noble metal. They also pointed out that tin oxide has no passivation effect and the contact resistance would increase progressively when tin is present in the metallization. However, metallizations of pure Cu and Pb were acceptable in high humid environments because oxides of Cu and Pb tend to form dense layers and further corrosion can be hindered.

Lu et al. [7] showed additional evidences supporting the electrochemical corrosion mechanism. They found that the joint resistance could keep stable either in dry environments or under the 85°C/85%RH condition but only one metal was involved.

Only if two different metals (e.g., Ni fillers and Ag wire) were involved, would the joint resistance increase dramatically. By formulating low moisture absorption resin and adding corrosion inhibitors, these authors succeeded in developing high-performance ICAs.

5.3.4.3 Formation of Intermetallic Compounds

Increase of resistance after environmental tests can also be attributed to the formation of intermetallic compounds. Yamashita and Suganuma [8] investigated the heat-induced degradation of the interface between ICA and SnPb-plated Cu electrode. Their element mapping analysis showed the apparent Sn diffusion into Ag particles. The occurrence of Ag–Sn intermetallic compounds, such as Ag_3Sn and Ag_4Sn, was identified in the X-ray diffraction pattern. They attributed this phenomenon to the Kirkendall diffusion of Sn from the plating layer into the Ag particles. At 150°C, the diffusion constant of Sn in Ag ($2.31 \times 10^{-17} m^2/s$) is much larger than that of Ag in Sn ($2.32 \times 10^{-20} m^2/s$). Therefore, the preferential diffusion of Sn occurs. This results in large Kirkendall voids in the SnPb plating layer, which decreases the true bonding area of the ICA joint and thus degrades both electrical and mechanical properties. These authors also pointed out that the diffusion constant of Sn in Ag_3Sn ($6.37 \times 10^{-12} m^2/s$) is even higher than that of Sn in Ag and the formation of Ag_3Sn cannot hinder the Kirkendall diffusion of Sn.

5.3.4.4 Filler Motion

Several researchers [9–12] have noticed the difference in deformation behaviors of metal fillers and polymer matrix. Typically conductive adhesive joints can sustain a shear strain of 10%, which is an order great than solders. But the metal fillers in ICA cannot be strained that much. Instead, they would move relatively to one another due to the compliancy of the matrix. Some possible influences on ICA reliability were proposed, concerning this situation.

Keusseyan et al. [9] observed that compliant adhesive joints could survive more than 3,000 thermal cycles without losing much mechanical strength, but the electrical resistance increased significantly. They suggested that relative movement among fillers, combined with viscoplastic deformation of matrix, would pull the insulating polymer in between fillers, leading to the loss of interfiller contacts.

With similar observations, Rörgren and Liu [10] suggested that the filler motion would result in sliding along the interface between fillers. When the adhesive joint is subject to cyclic loadings, this interfacial sliding would eventually wear out the direct contact points among fillers and degrade the electrical performance of the ICA joint in the long run. Besides filler friction, the numeric simulation [11] showed that stress concentration due to filler motion would promote the initiation of microcracks in polymer matrix, which could weaken the constraint on fillers, loosen their intimate contacts, and therefore increase the bulk resistance.

Constable et al. [12] performed mechanical low cycle fatigue tests on several ICA joints and measured the resistance changes with a highly sensitive micro-ohm technique. The resistance was observed to increase apparently at the initiate stage of the tests, while the force required for the same deformation amplitudes decreased gradually. The authors attributed this phenomenon to the formation of wear tracks from filler frictions. However, they insisted that the influence of filler motion is limited and the dominant failure mechanism is interfacial fracture of the joint.

5.3.4.5 Ag Migration

In the presence of water and an electric field, silver is anodically dissolved at its original location and moves toward the cathode where it is deposited. This migration phenomenon can lead to the growth of dendrites between adjacent electrodes and lower the surface insulation resistance (SIR) of the board. For many years, the short circuit due to Ag migration has been a nuisance to those using silver inks and similar.

However, due to that the silver fillers are encapsulated with an epoxy layer, Ag migration is not likely to occur in conductive adhesives under test conditions relevant in practice, e.g., 85°C/85%RH or 60°C/90%RH under 5 V bias [2]. But under more severe conditions, such as the presence of a liquid water film, higher bias and smaller pitch spacing, Ag migration does occur. For example, short circuit between 8-mil spaced pads has been observed after 2,000 h of 85°C/85%RH test with 15 V bias (Fig. 5.5). In ref. [13], the migration of Ag particles was also observed in ICA joints subjected to the current-induced aging (10–30 A) and the consequent electrical degradation was reported.

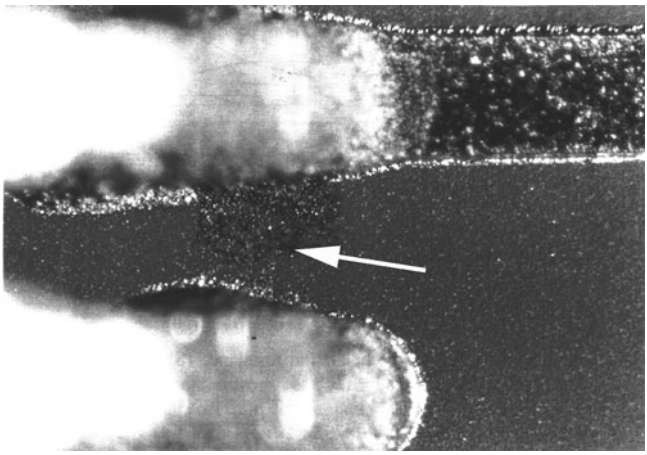

Fig. 5.5 Ag migration between 8-mil spaced pads after 2,000 h of 85°C/85%RH test with 15 V bias

5.3.5 *Electron Conduction Through Nanoparticles in ICA*

High metal loading, in the range of 20–35 vol% is normally required to guarantee effective electrical conduction of ICA joints, which results rather often in adhesive failure. Based on the percolation theory, ICAs using a bimodal distribution of metal fillers were expected to have a decreased metal loading for better mechanical performance while the electrical property remains unchanged [14]. It was, however, demonstrated experimentally that the electrical conductivity has been reduced when the volume percentage of the nanosize fillers in the system was increased [15]. To explain this phenomenon, the electron conduction through nanoparticles in a normal ICA was investigated based on quantum-mechanical considerations [16].

Consider a substructure in the ICA that consists of one nanoparticle sandwiched between two microparticles (Fig. 5.6).

For the nanoparticle between the two microparticles, the quantum confinement effects must be included. Using the uniform background model, the ground sublevels across the substructure are approximately:

$$E_{nm}(z) = \frac{\pi^2 \hbar}{2r(z)^2 m_0}(n^2 + m^2), \tag{5.1}$$

where $r(z)$ is the radius of the cross section at z, n and m are nonzero integers. The ground sublevel $E_{11}(z)$ is also presented in Fig. 5.6, where a potential barrier in the nanoparticle side of the interconnect ($z = 0$) between the micro- and nanoparticles is observed.

When the structure is biased by V_{ex}, the local Fermi level of the left microparticle is kept unchanged (assumed to be grounded). The local Fermi level of the other microparticle becomes $E_f + eV_{ex}$, its conduction band edge E_{11} is also lifted up by an amount of eV_{ex}. The time-dependent quantum mechanical behavior of an electron can be described by its wave packet. As the electron transports through the substructure of Fig. 5.6 from left to right, the electron wave packet is split into two parts after

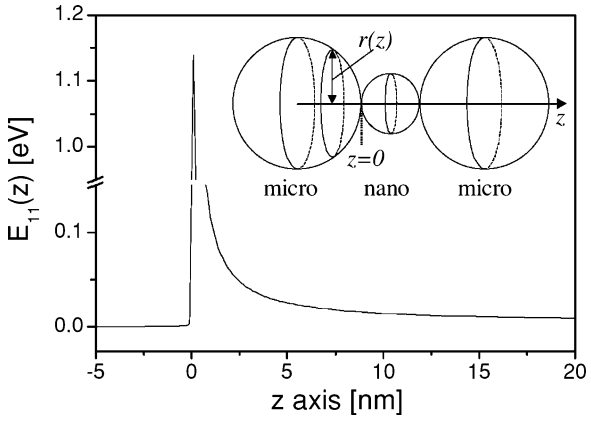

Fig. 5.6 Schematics of a micro–nano–micro substructure in ICA and the potential energy profile at the interconnect between the micro- and nanoparticles

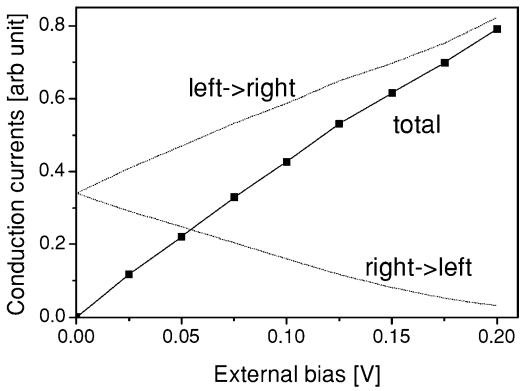

Fig. 5.7 Current–voltage characteristics of the micro–nano–micro substructure

reaching the left interconnect energy barrier at $z = 0$. One is reflected back, and the other tunnels through the nanoparticle. Calculation shows that, due to the barriers, only half of the initial electron gets transmitted through the nanoparticle. This qualitatively agrees with experimental observations that the electrical conductivity has been reduced as nanosize fillers are added into the ICA.

The current–voltage characteristics of such a structure are presented in Fig. 5.7. The total current is obtained by subtracting the reflected current from the transmitted current. Increasing the external bias effectively lowers the energy barriers so that the transmitted current increases; however, it lifts up the conduction band edge E_{11} of the left microfiller so that the reflected current decreases considerably. The final total current through the substructure in general increases linearly in the external bias range under investigation.

5.4 Reliability of ACA Interconnects

Recent environmental legislation has led to an increasing interest in the possibility of substituting ECAs for the traditional tin–lead solders in electronics manufacturing. The conductive adhesives mentioned in this chapter are composites of insulating polymer matrix and conductive fillers. Depending on the loading of fillers, conductive adhesives can be cataloged as ICA and ACA. In this section, our topic focuses on the ACA. ACA is a new class of adhesives that are conductive in one direction, which offers the following advantages over traditional tin–lead solders in the interconnections.

- Low-temperature processing
- Compatibility with a wide range of substrates
- No flux pretreatment or postcleaning procedures required
- No lead or other toxic metals
- Finer pitch capability
- Solder mask not required

ACAs are prepared by dispersing conductive fillers in an adhesive matrix. The unidirectional conduction is achieved by using a relatively low volume fraction of conductive fillers. This low filler loading is insufficient for interparticle contact and prevents conduction in the *X*–*Y* plane of the adhesive, but enough particles are present to assure reliable conduction between bonding electrodes in the *Z*-direction. Because of the anisotropy, ACAs can be deposited over the entire contact region, greatly expanding the bonding area. Also the low filler loading improves the bonding strength. Thus, mechanically robust interconnection can be achieved with ACA assembly.

ACAs come in two distinct forms: paste and film. Pastes can be printed with screen or stencil or dispensed with a syringe. Films are supplied by manufacturers on reel and are extremely suitable for nonplanar bonding surfaces. Both thermoplastic and thermosetting resins have been used as adhesive matrices. The principal advantage of thermoplastic ACAs is the relative ease to disassemble the interconnections for repair operation, while thermosetting adhesives possess higher strength at elevated temperature and form more robust bonds [17]. The commonly used conductive fillers include silver and nickel particles and polymer spheres coated with metal (Ni/Au). Silver particles offer moderate cost, high electrical conductivity, and low chemical reactivity. Nickel particles can break the oxide layer on the electrodes and are suitable for interconnecting easily oxidized metal. Metal-coated polymer spheres have fairly uniform diameter distributions. They can provide high interconnection reliability because of the large elastic deformation during bonding. Recent application of solder particles as ACA fillers has also been reported [18].

Since the conduction of ACAs is based on mechanical particle–electrode contacts, pressure is a requisite to form qualified joints. A typical ACA assembly is shown in Fig. 5.8. After alignment, pressure is applied on the backside of the chip. The adhesive resin is squeezed out and conductive particles are trapped and deformed between opposing electrodes. Once electrical continuity is generated, the adhesive resin is cured with heat or UV. The intimate particle–electrode contacts are maintained by the cured matrix and the elastic deformation of particles, and electrodes exert a continuous contact pressure.

ACA interconnection finds particular applications with fine-pitched flip-chip techniques used to mount bare chip on various substrates such as ITO-coated

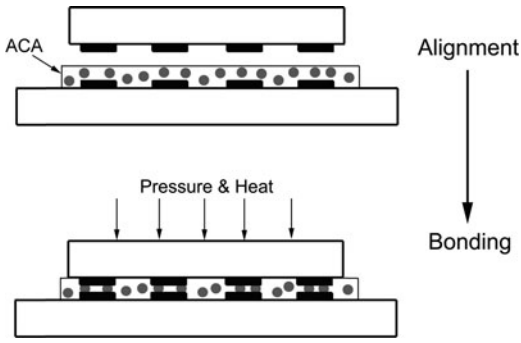

Fig. 5.8 Manufacturing process of ACA assembly

glass, FR4 board, and flexible films. ACA joining is also attractive for fine-pitched surface mount component assembly. However, the performance and reliability of ACA joints are more sensitive to the joint design, substrate/component properties, and process conditions than solder joints.

5.4.1 *Effects of Assembly Process*

The assembly process of ACA interconnection includes alignment, bonding and, if solder interconnects exist in the same board, reflow. Due to the low surface tension, ACA interconnection lacks the benefit of the self-alignment, which put a stringent requirement on the alignment accuracy. A normal flip-chip bonder that offers a ± 5 μm accuracy is normally good enough. Nevertheless, bad alignment would result from incorrect operations. It can influence the pressure distribution and, in more serious situations, decrease the contact area for electrical interconnection (Fig. 5.9).

The bonding process is very critical to the ACA joint performance and reliability, since both mechanical integration and electrical interconnection are established in this process. Bonding pressure and temperature are the two most important parameters. To achieve reliable ACA joints, adequate bonding pressure should be applied uniformly and suitable bonding temperature should be kept for sufficient time.

The bonding pressure is applied to force the conductive particles to contact the electrodes. The performance of the joint depends heavily on the deformation degree of particles. Ideally, the particles should be squashed enough to gain the largest contact area. However, the integration of particle body should be maintained and cracking due to over pressure could degrade the electrical performance.

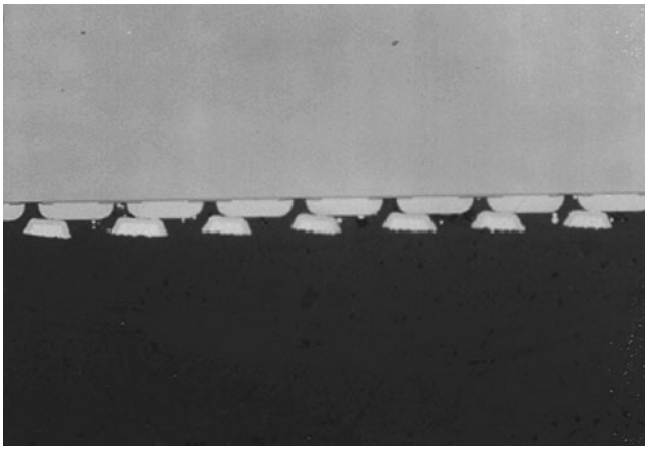

Fig. 5.9 Bad alignment degrades the electrical performance and reliability of ACA joints

It is also important to keep the pressure uniform during the bonding. Nonhomogeneous bonding pressure can cause particles being deformed unevenly, which could result in poor long-term reliability. This problem becomes more serious for thin and flexible substrates.

The effects of particle deformation on joint electrical reliability during temperature cycling are summarized schematically in Fig. 5.10. Type 1 represents the best case where the particles are deformed uniformly and atomic bonding between the particles and contacts is achieved. Type 2 joints consist of undeformed or slightly deformed particles due to either low bonding pressure or inhomogeneous pressure distribution. The conductive character of these joints is unstable at high temperature because the epoxy matrix will expand more than the particles. Type 3 joints can

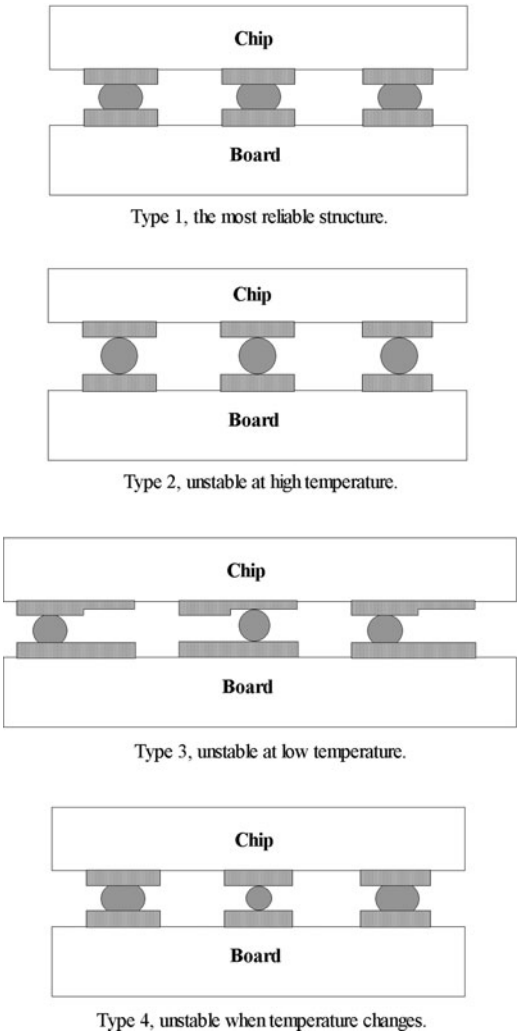

Fig. 5.10 Schematics of four types of ACA joints caused by variations in bonding pressure, bump geometry, and filler size

result from shape or height variations of the contact areas. Some particles are not deformed enough and will shrink more than those well deformed, causing problems at low temperature. Finally, type 4 pictures a uniform height of the contact areas, but a very large variation of particle size. Due to the weak bonding between the smaller particles and contact area, electrical opens can be observed at both low and high temperatures. All these situations have been observed experimentally.

The bonding temperature and time heavily influence the curing degree of the adhesive that plays an important role in the reliability of ACA joints. In the under-cured joint, the cross-linkage of the polymer may be incomplete and neither mechanical performance nor electrical reliability can be guaranteed under high humidity tests. To gain a certain curing degree, longer bonding time should be employed with lower bonding temperature. However, this is not preferable due to the low productivity. On the other hand, too high bonding temperature is not desired, either. This is because the epoxy may solidify too quickly and hence the conductive particles would not have enough time to distribute themselves in between the bumps and pads. Recent work also observed the chain scission due to high bonding temperature. So finding the optimum combination of bonding temperature and time is a fundamental step toward reliable ACA interconnection.

If ACA interconnection is used together with soldering technology for the final products, reflow soldering after ACA bonding is inevitable. During reflow, the package needs to be heated up to above 200°C, which is much higher than the normal bonding temperature of ACA joint. The ability of ACA interconnection to withstand this high temperature is critical for successful packaging. Yin et al. [19] found that the contact resistance of ACA joints increased significantly after reflow process and conduction gaps formed between the conductive particles and the electrode. Seppälä and Ristolainen [1] also reported the detrimental effects of reflow on the reliability of ACA joints. The possible reason is that, due to its much higher coefficient of thermal expansion (CTE), the adhesive matrix expands in the *Z*-direction much more than the particles during the reflow. The induced thermal stress lifts the chip from substrate and damages the bonding structure. Therefore, the peak temperature of reflow profile and the distance between the chip and substrate (related to bump height) are the most important factors. By optimizing process parameters and adopting ACA with lower CTE, the effects of the reflow process can be reduced to some extent.

5.4.2 Effects of Substrate and Component

Suitable substrate stiffness and bump dimensions are also important to achieve reliable ACA joints. With a soft substrate, significant deformation of the substrate may occur during the bonding, which has a direct influence on the joint quality. On the FR4 board, it was observed that the electrical resistance and reliability of a joint depend on the distance between the pad and glass fibers in the substrate (Fig. 5.11). A long distance means a thick layer of soft epoxy that may deform during bonding. Therefore, enough particle deformation cannot be obtained at that point.

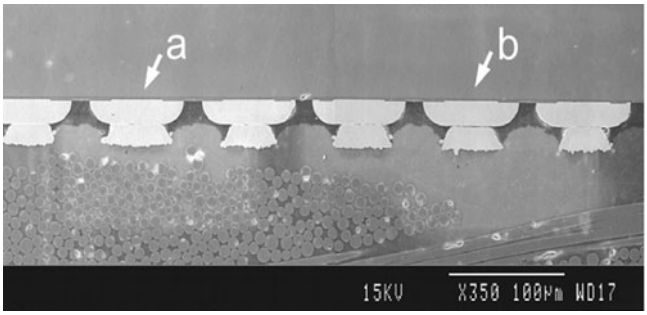

Fig. 5.11 Electrical resistance and reliability of a joint depend on the distance between the pad and glass fibers in the substrate. Joint **a** has a better electrical performance than joint **b** (5 vs. 14 mΩ) due to its location closer to glass fibers

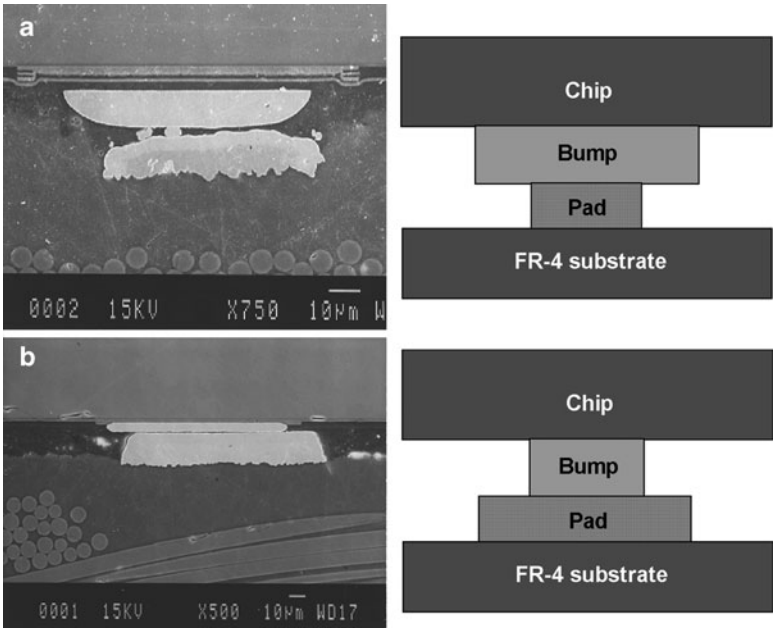

Fig. 5.12 (**a**) Pad sinking leads to insufficient particle deformation and (**b**) using a bump smaller than the pad can decrease pad sinking

Figure 5.12a shows that large force exerted on the pad causes the pad sinking and almost no deformation occurring in the particles. An approach to reduce the pad sinking is to use a relatively smaller bump area compared with the pad area. Therefore, less bonding force will be transferred to the pad as shown in Fig. 5.12b.

For flip-chip solder joining, plastic strain of solder bumps is a critical parameter that governs the joint reliability. Using a high bump can reduce the bump strain and thus increase the joint reliability, as shown in Fig. 5.13a. However, a systematic

Fig. 5.13 (**a**) Using high bumps can reduce the strain of solder joints, but (**b**) it has much less influence on the strain of ACA joints

study of the effect of bump height showed that the failure mechanism of ACA flip-chip joints is totally different. In ACA joints, the bump and pad are usually made of metals that are much stiffer than adhesives. In other words, thermal mismatch stresses can hardly deform the bump and pad, and the shear strain is localized in the adhesive between the mating bump and pad (Fig. 5.13b). In this case, the joint reliability is governed by the shear strain in the adhesive and the influence of bump height is limited. Meanwhile, the stress in the *Z*-axis will be raised with bump height due to the increased adhesive volume. At elevated temperature, this stress can lift the chip and weaken the joint. So benefits from high bumps cannot be expected for ACA joints. Another practical problem associated with high bumps is that air bubbles are easily introduced during ACA bonding.

5.4.3 Degradation Due to Moisture Absorption

ACAs contain a much larger quantity of polymers. Therefore, polymer degradation due to moisture absorption becomes more significant in ACA joints. Water can degrade polymers through (1) depression of the glass transition temperature T_g and functioning as a plasticiser, (2) giving rise to swelling stresses, and (3) generating voids or promoting the catastrophic growth of voids already present. All three occurrences have been known to lead to mechanical degradation. Moisture absorption can also contribute to the disruption of conductivity in the path between mating electrodes. This may include, for example, changes in the polymer/filler dispersion state through the expansion of the polymer matrix and formation of defects such as cracks and delaminations.

The effects of moisture on an ACA film was studied with Fourier transform infra-red (FTIR) spectra that provide a vast reservoir of molecular information pertaining to the chemical groups present, as well as to the structure arrangement and bonding preferences of these groups. The adhesive was conditioned in two environments: 85°C/85%RH and 22°C/97%RH. After certain amount of time, samples were taken out of the chamber and FTIR spectra were collected.

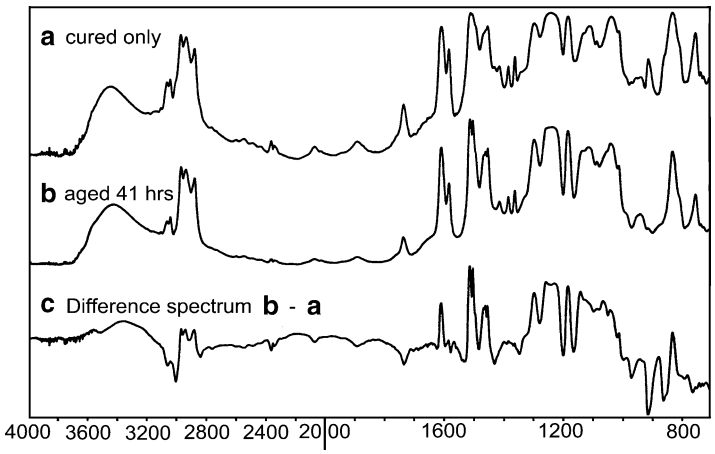

Fig. 5.14 FTIR spectra of an ACA film (**a**) after curing; (**b**) aged at 85°C/85%RH for 41 h, and (**c**) the difference spectrum (**b–a**)

Figure 5.14 shows the spectra of the adhesive (a) after curing, (b) after 41 h exposure to 85°C/85%RH, and (c) the difference spectra representing the changes due to the moisture exposure. As shown, the negative bands at 868, 916, 1,345, 3,005, and 3,058/cm indicate the further progress of the cure reaction. Moisture degradation is believed to occur by hydrolysis of the ester linkages, which creates two end groups: a hydroxyl and a carbonyl. Though it is hard to see any new emerging carbonyl groups in this figure, the band at 3,560/cm indicates the existence of free hydroxyls. With more time exposure, curing effect is not observed, but degradation becomes more apparent. The spectra collected from samples exposed to 22°C/97%RH showed that moisture absorption through hydrogen bonding, but neither further curing nor degradation is observed, implying that the dominant degradation is associated with heat.

5.4.4 Oxidation and Crack Growth

To correlate the electrical resistance shift as a function of humidity test time, a theoretical model has been developed. It takes into account both oxidation and cracking, two primary failure mechanisms of conductive adhesive joints and can thus explain the experimental observations quite well (Fig. 5.15).

Before exposure to the humid environment, the initial resistance through the joint is:

$$R_{init} = R_s + R_j + R_l, \tag{5.2}$$

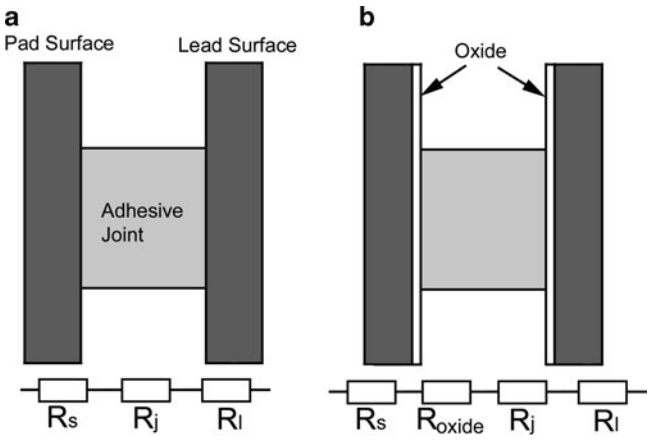

Fig. 5.15 Electrical conducting path through a conductive adhesive joint (**a**) before and (**b**) after humidity exposure

where R_s is the resistance through the substrate, R_j the resistance through the adhesive joint, and R_l the resistance through the component lead. After the humidity test, the joint resistance becomes:

$$R_{after} = R_s + R_j + R_l + R_{oxide} = R_{init} + R_{oxide}, \tag{5.3}$$

where R_{oxide} is the resistance through the oxide layer which can be expressed as:

$$R_{oxide} = \rho_{oxide} \frac{L}{A}, \tag{5.4}$$

where ρ_{oxide} is the volume resistivity of the oxide layer, L the oxide layer thickness, and A the contact area.

Since polymer structures normally contain a large amount of free volume, it is reasonable to assume that the diffusion of oxygen is much faster in polymers than in metal oxides. In other words, the oxygen diffusion through the oxide layer will control the oxide growth rate and consequently the increase of the resistance in the oxide layer.

Assume the following Einstein equation holds:

$$L = \sqrt{2D_{oxide}t}, \tag{5.5}$$

where D_{oxide} is the diffusion parameter of oxygen through the oxide layer and t is the time for the oxygen diffusion. Combining (5.3)–(5.5), one can obtain the relationship between the time and the resistance change:

$$\frac{R_{after}}{R_{init}} = 1 + \frac{L_e \rho_{oxide}}{AR_{init}} \sqrt{\frac{t}{t_e}}, \tag{5.6}$$

where L_e is the oxide layer thickness at the end of test, t the elapsed time, and t_e the total test time. Equation (5.6) can be used to calculate the relative electrical resistance change due to oxidation.

The crack normally occurs at the interface between the adhesive and the electrode and decreases the real contact area gradually. Here assume the contact area A can be expressed as:

$$A = A_0\left(1 - \frac{t}{t_e}\right), \tag{5.7}$$

where A_0 is the original contact area. Therefore, taking into account the crack growth, the electrical resistance change becomes:

$$\frac{R_{after}}{R_{init}} = 1 + \frac{L_e \rho_{oxide}}{A_0(1 - t/t_e)R_{init}}\sqrt{\frac{t}{t_e}}. \tag{5.8}$$

Figure 5.16 shows the calculated results with (5.6) and (5.8), using the parameters given in Table 5.1. The calculations show that if no crack is formed, the electrical resistance will increase gradually with test time, but no catastrophic failure will be expected. The effect of cracking is rather small at the beginning, but then becomes more and more significant with the increase of test time. If a complete crack forms by the end of the testing, the electrical resistance will go to infinity.

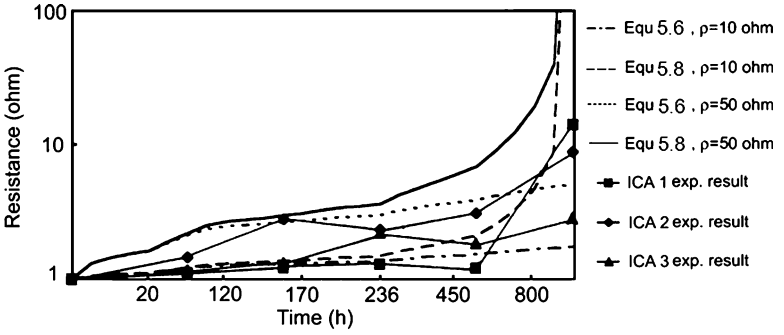

Fig. 5.16 Calculated and observed results of electrical resistance change as a function of humidity test time for ICA joints on copper surfaces

Table 5.1 Parameters used for calculation of the resistance evolution of an adhesive joint at 85°C/85%RH

Bonding surface	Oxide	Oxide (m)	A_0 (μm^2)	L_e (nm)	Dioxide (m^2/s)	R_{init} (−)
Copper	Cu_2O	10–50	1.1×10^{-6}	20	5×10^{-20}	0.2

For comparison, the experimental results obtained earlier are also given in Fig. 5.16. Before 500 test hours, (5.6) can predict the experimental observations quite well. However, the experimental results after 500 h cannot be explained by considering the oxidation of copper metal surface only, which means that fracture must have taken place during the humidity testing. In fact, cracks have already been observed after 158 h of exposure.

5.4.5 *Probabilities of Open and Bridging*

If the ACA contains insufficient particles, there is of course a certain probability that no particle exists in the joint and an open is resulted. On the other hand, bridging is possible due to there being too many particles in a too short spacing, causing short circuit between neighboring pads. Accurately estimating probabilities of open and bridging is important to explore the limiting pitch of ACA interconnection at which the open/short circuit probability becomes unacceptable (Fig. 5.17).

Mannan et al. proposed an analytical method to estimate the open probability. Assume that the number of particles on a pad obeys Poisson distribution:

$$P(n) = \frac{e^{-\mu}\mu^n}{n!}, \tag{5.9}$$

where $P(n)$ is the probability of finding n particles on a pad and μ is the average number of particles on a pad. If the volume fraction of particles f and the particle radius r are known, μ is given by:

$$\mu = \frac{3Af}{2\pi r^2}, \tag{5.10}$$

where A is the pad area. Thus the probability for an open ACA joint is:

$$P(0) = e^{-\mu} = e^{-3Af/2\pi r^2}. \tag{5.11}$$

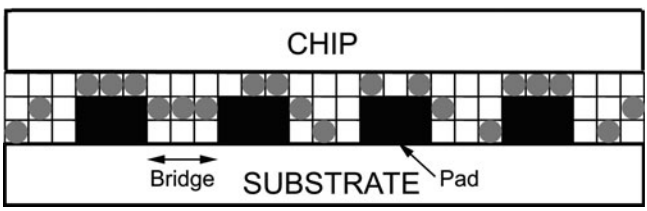

Fig. 5.17 Schematics of bridging in the ACA interconnection [20]

For a typical ACA with a volume fraction of particles ranging from 3 to 15 vol%, the open circuit probability on a 100 μm^2 pad varies from 10^{-13} to 10^{-3}, which is extremely small. However, in reality, there is always a crowding effect that must be taken into account. In this case, the particle distribution can be described using a binominal distribution model:

$$P(n) = C_n^N (1-s)^{N-n} s^n, \tag{5.12}$$

where N is the maximum number of particles that can be contained in the pad area A. C_n^N is the binominal coefficient and s is equal to f/f_m where f_m is the volume fraction corresponding to maximum packing. In the limit that $f \ll 1$, (5.11) and (5.12) give identical results for $P(0)$.

For a rough estimation of bridging, Mannan et al. proposed a simplified box model. As shown in Fig. 5.18, the volume between pads can be divided into cubic boxes with sides the same length as the particle diameter. If k boxes are filled out of a total of N, the volume fraction of particles is:

$$f = \frac{k4/3\pi r^3}{N(2r)^3}, \tag{5.13}$$

where r is the particle radius. Thus the probability for a single box being occupied is given by:

$$\frac{k}{N} = \frac{6f}{\pi}. \tag{5.14}$$

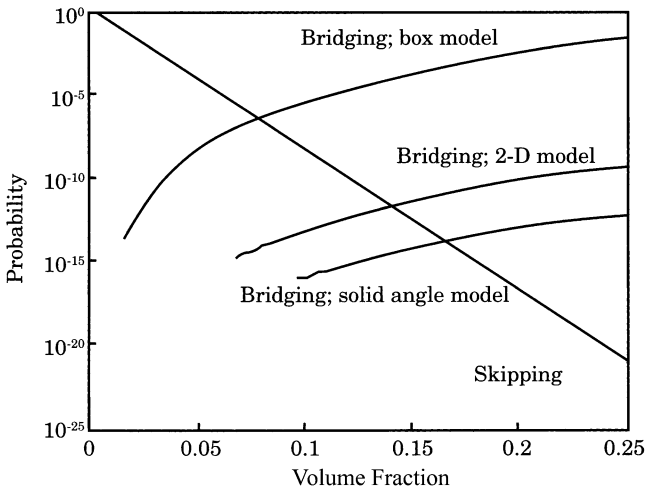

Fig. 5.18 Probability of particles bridging gap as a function of filler volume fraction [20]

Determined by the number of boxes that can be fitted onto the side of a single pad and by $(6f/\pi)^q$ where q is the lowest number of particles needed to bridge the pad spacing, the bridging probability is given by:

$$p = 1 - \left(1 - \left(\frac{6f}{\pi}\right)^{d/4r^2}\right)^{hl/4r^2}, \tag{5.15}$$

where h and d are the pad height and length, respectively, and l is the spacing between the pads.

This box model only gives an upper limit. Figure 5.18 shows the bridging probabilities derived from different models. It is clear that the lowest combined probability for bridging and skipping occurs in the volume fraction between 7 and 15%, depending on which model is used. This volume fraction range is also generally used for commercial ACA materials today.

5.4.6 ACA Flow During Bonding

As modeled by Mannan et al. [20], there are two types of adhesive flow during the ACA bonding (Fig. 5.19). Type 1 flow occurs around individual pads and bumps at the beginning of bonding, filling voids nearby. After voids are completely filled, type 2 flow becomes dominant, expelling the adhesive from under the chip to edges.

By solving the Navier–Stokes equations of Newtonian fluid, one can obtain the following equation that describes the pressure distribution under the chip in the cylindrical coordinate system:

$$P(r) = \frac{2F}{\pi R^2}\left(1 - \frac{r^2}{R^2}\right), \tag{5.16}$$

where R is half of the side length of the chip and F is the bonding force. In reality, the ACA resin probably behaves more like power law fluids:

$$\tau_{xy} = \eta_0\left(\frac{d\gamma}{dt}\right)^n, \tag{5.17}$$

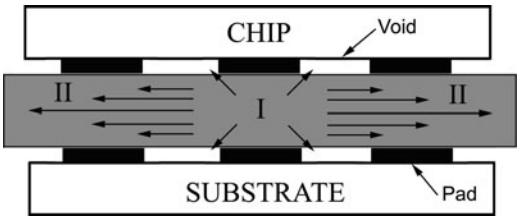

Fig. 5.19 The ACA flow during the bonding [20]

where η_0 is termed the consistency and n the power law index. For a Newtonian fluid, n equals 1 and η_0 becomes the viscosity of the fluid. As the chip is pressed down, the ACA is squeezed out between the chip and substrate. With power law fluids, the process time t_p for reducing the gap height from h_0 to h_1 is given by:

$$t_p = \frac{2n+1}{n+1}\left(\frac{2\pi\eta_0 R^{n+3}}{F(n+3)h_0^{n+1}}\right)^{1/n}\left(\left(\frac{h_0}{h_1}\right)^{(n+1)/n} - 1\right). \tag{5.18}$$

This process time is important to determine the suitable heating ramp for bonding. Too high bonding temperature may cause the adhesive solidify before particles are deformed completely, resulting in less reliable joints.

5.4.7 *Electrical Conduction Development and Residual Stresses*

As ACAs contain a small volume fraction of particles, there is no conduction in any direction before bonding. The electrical resistance starts to decrease as pressure increases due to enlarged contact area. Several research groups have reported the deformation effect on the electrical conduction development during the ACA assembly. The first publication is from Williams et al. [21] and the contact resistivity ρ of an ACA joint was estimated as:

$$\rho = \frac{A\rho_B\left(\sqrt{6\pi n\kappa/\sigma A} - (1/R_B)\right)}{4\pi n R_B}, \tag{5.19}$$

where ρ_B is the resistivity of the conductive particle, n is the number of contacts within the contact area A, κ is the shear yield stress of a conductive particle with a radius of R_B, and σ is the pressure applied to the joint.

With a combination of analytical method and FEM, Hu et al. [5] derived the relationship between the resistance and bonding pressure both for the rigid and deformable particle systems, as shown in Fig. 5.20. They also simulated the contact between the particle and electrode with FEM. As shown in Fig. 5.21, significant compressive stress is found to build up in the interface between the two contacts. This stress is believed to generate peel stress in the adhesive, which is probably the reason for catastrophic failure.

Fu et al. [6] considered the multiparticle case and found that the particle location in an ACA joint can affect its electric conductance. As shown in Fig. 5.22, a particle in the center of the joint contributes much more to the electrical performance than a particle close to the edge of the joint. This helps to explain why the measured resistance scatters greatly from one joint to another. Increasing the number of particles on the contact pad can improve the uniformity of the electric conduction.However, it also increases the constriction resistances due to fellow particles. So the total conductance does not increase in an additive manner.

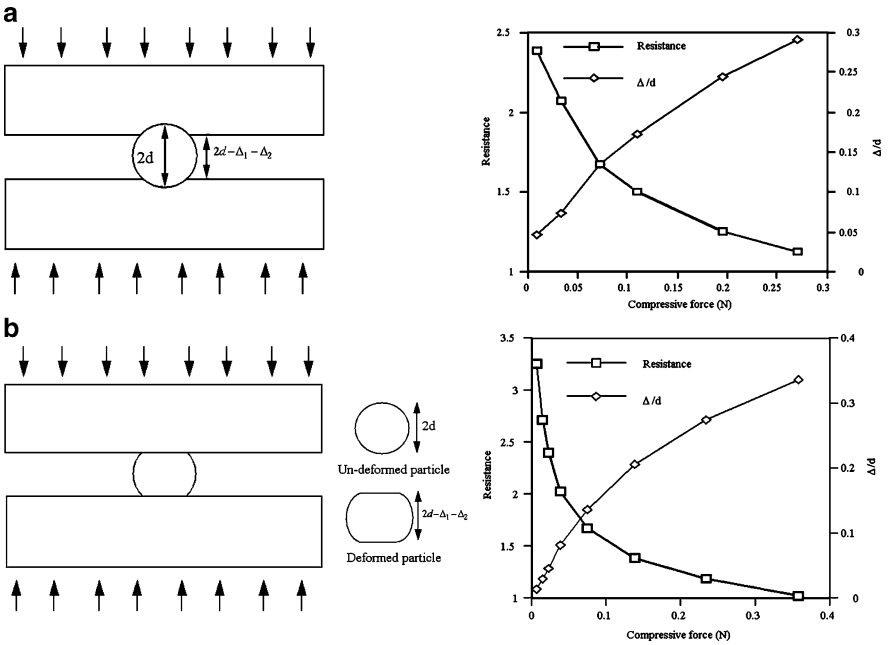

Fig. 5.20 Force–resistance–deformation relationships for (**a**) rigid particle system and (**b**) deformable particle system (courtesy of C.P. Yeh)

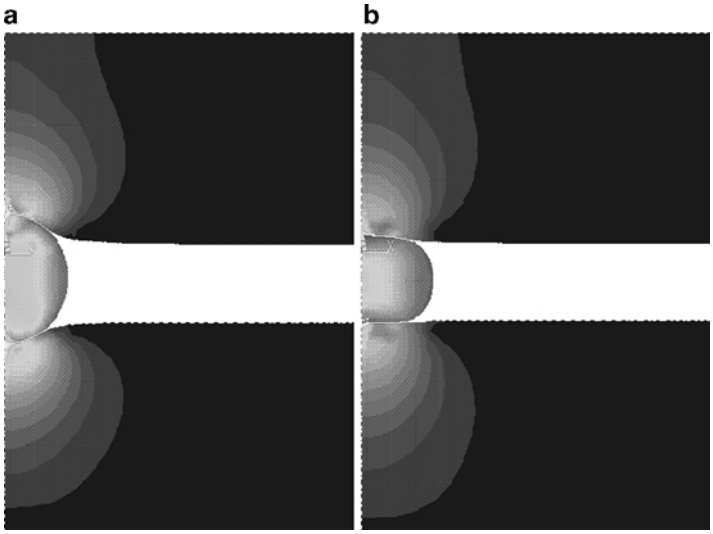

Fig. 5.21 Deformation distributions of (**a**) rigid particle system and (**b**) deformable particle system (courtesy of C.P. Yeh)

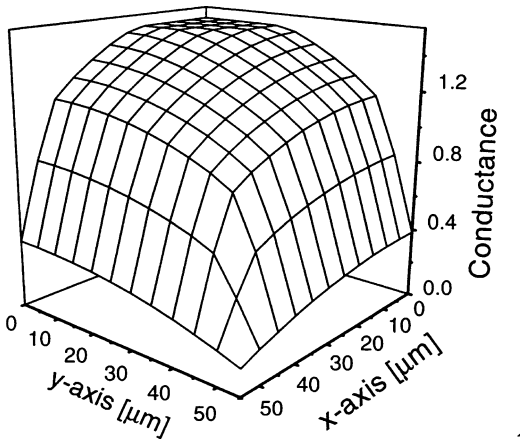

Fig. 5.22 Electric conductance of the particle as a function of its location away from the center of the ACA joint

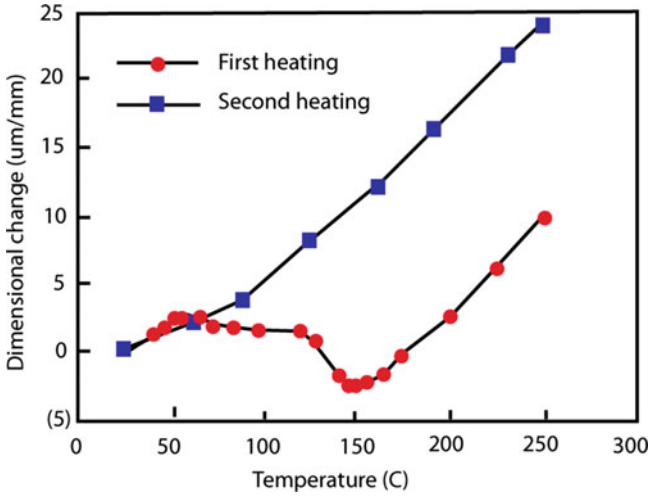

Fig. 5.23 Dimensional change of conductive adhesive

Exercises

5.1 Figure 5.23 shows the dimensional change during cure of a conductive adhesive. How can estimate the curing shrinkage from the curve. If the original sample is 60-μm long and the shrinkage is isotropic, what is the shrinkage value in this case?

5.2 What are the advantages of conductive adhesives comparing to traditional tin–lead solders?

5.3 For a thermal-setting conductive adhesive, the cure reaction can be expressed by Arrhenius equation as:

$$\frac{dx}{dt} = Z \exp\left(-\frac{E_a}{RT}\right)(1-x)^n.$$

The preexponential is 3.23×10^{14}/s, the activation energy is 106.4 kJ, R is gas constant as 8.314 J/mol/K. Assuming the curing reaction is second order, at least how long time should we hold it at 140°C before it is fully cured (99.99%)?

5.4 Why is Coffin–Manson relationship more suitable for solder joints and why is Morrow's law more suitable for conductive adhesive joints?

5.5 Why using higher bumps in the conductive adhesive joints cannot get a similar result in low cycle fatigue tests?

References

1. H. Botter, R. B. Van Der Plas and A. Arunjunai, "Factors that Influence the Electrical Contact Resistance of Isotropic Conductive Adhesive Joints During Climate Chamber Testing", International Journal of Microelectronic Packaging Materials and Technologies, 1, 1998, 177–185.
2. J. C. Jagt, "Reliability of Electrically Conductive Adhesive Joints for Surface Mount Applications: A Summary of the State of the Art", IEEE Transactions on Components Packaging and Manufacturing Technology Part A, 21, 1998, 215–225.
3. S. Y. Xu and D. A. Dillard, "Determining the Impact Resistance of Electrically Conductive Adhesives using a Falling Wedge Test", IEEE Transactions on Components and Packaging Technologies, 26, 2003, 554–562.
4. M. G. Perichaud et al., "Reliability Evaluation of Adhesive Bonded SMT Components in Industrial Applications", Microelectronics Reliability, 40, 2000, 1227–1234.
5. L. Li et al., "Reliability and Failure Mechanism of Isotropically Conductive Adhesives Joints", 45th Electronic Components and Technology Conference (ECTC), Proceedings, Las Vegas, NV, IEEE CPMT Society, 1995, 114–120.
6. S. Y. Xu, D. A. Dillard and J. G. Dillard, "Environmental Aging Effects on the Durability of Electrically Conductive Adhesive Joints", International Journal of Adhesion and Adhesives, 23, 2003, 235–250.
7. D. Lu, Q. K. Tong and C. P. Wong, "Mechanisms Underlying the Unstable Contact Resistance of Conductive Adhesives", IEEE Transactions on Electronics Packaging Manufacturing, 22, 1999, 228–232.
8. M. Yamashita and K. Suganuma, "Degradation Mechanism of Ag-Epoxy Conductive Adhesive/Sn-Pb Plating Interface by Heat Exposure", Journal of Electronic Materials, 31, 2002, 551–556.
9. R. L. Keusseyan, J. L. Dilday and B. S. Speck, "Electric Contact Phenomena in Conductive Adhesive Interconnections", International Journal of Microcircuits and Electronic Packaging, 17, 1994, 236–242.

10. R. S. Rörgren and J. Liu, “Reliability Assessment of Isotropically Conductive Adhesive Joints in Surface-Mount Applications”, IEEE Transactions on Components Packaging and Manufacturing Technology Part B, 18, 1995, 305–312.
11. Z. M. Mo et al., “Electrical Characterization of Isotropic Conductive Adhesive under Mechanical Loading”, Journal of Electronic Materials, 31, 2002, 916–920.
12. J. H. Constable et al., “Continuous Electrical Resistance Monitoring, Pull Strength, and Fatigue Life of Isotropically Conductive Adhesive Joints”, IEEE Transactions on Components and Packaging Technologies, 22, 1999, 191–199.
13. H. K. Kim and F. G. Shi, “Electrical Reliability of Electrically Conductive Adhesive Joints: Dependence on Curing Condition and Current Density”, Microelectronics Journal, 32, 2001, 315–321.
14. Y. Fu, J. Liu and M. Willander, “Conduction Modelling of a Conductive Adhesive with Bimodal Distribution of Conducting Element”, International Journal of Adhesion and Adhesives, 19, 1999, 281–286.
15. L. Ye et al., “Effect of Ag Particle Size on Electrical Conductivity of Isotropically Conductive Adhesives”, IEEE Transactions on Electronics Packaging Manufacturing, 22, 1999, 299–302.
16. Y. Fu and J. Liu, “Electron Conduction through Nano Particles in Electrically Conductive Adhesives”, Micromaterials and Nanomaterials, 4, 2004, 104–109.
17. D. Klosterman, L. Li and J. E. Morris, “Materials Characterization, Conduction Development, and Curing Effects on Reliability of Isotropically Conductive Adhesives”, IEEE Transactions on Components Packaging and Manufacturing Technology Part A, 21, 1998, 23–31.
18. A. J. Lovinger, “Development of Electrical-Conduction in Silver-Filled Epoxy Adhesives”, Journal of Adhesion, 10, 1979, 1–15.
19. J. Liu et al., “Surface Characteristics, Reliability, and Failure Mechanisms of Tin/Lead, Copper, and Gold Metallizations”, IEEE Transactions on Components, Packaging, and Manufacturing Technology Part A, 20, 1997, 21–30.
20. S. W. Kim, J. W. Yoon and S. B. Jung, “Interfacial Reactions and Shear Strengths Between Sn-Ag Based Pb-free Solder Balls and Au/EN/Cu Metallization”, Journal of Electronic Materials, 33 (10), 2004, 1182–1189.
21. A. Sharif, Y. C. Chan, M. N. Islam and M. J. Rizvi, “Dissolution of Electroless Ni Metallization by Lead-Free Solder Alloys”, Journal of Alloys and Compounds, 388(1), 2005, 75–82.